University of Crete
Department of Computer Science

University Joseph Fourier
Department of Computer Science
and Applied Mathematics

Institute for Engineering
and Health Information

Image-Guided Brachytherapy Robot

Master Thesis

Aretopoulou Despoina

Heraklion, July 2010

Image-Guided Brachytherapy Robot

Aretopoulou Despoina
MSc Student in Informatics,*
University Joseph Fourier, Grenoble 1
Laboratory TIMC, Equipe GMCAO
In3S, Medical Faculty
38706 La Tronce
France

Supervisors: Jocelyne Troccaz (Jocelyne.Troccaz@imag.fr),
Michael Baumann (michael.baumann@imag.fr)

24 June 2010

External expert: Simon Le Floch
Option responsable: Frank Hetroy

Permanents panel members: James Crowley,
Florence Maraninchi,
Laurent Mounier

*Master Franco-Hellenic in Informatics, University of Crete, Heraklion, Greece

Thanks to my parents, Ilias and MoSIG people!

Acknowledgements

I would like to thank profoundly my supervisors Jocelyne Troccaz, Michael Baumann and Nikolai Hungr for their generous guidance and insightful discussion regarding the context of the report.

I would also like to thank all the members of the team GMCAO, the PhD students and the Msc students for providing an excellent working environment. It was a great experience for me to perform my research with this team.

Finally, I wish to express my sincere thanks to Saddek Bensalem, the coordinator of the Master Franco-Hellenique in Grenoble and to Vassilis Christophides, the coordinator of the Master Franco-Hellenique in Heraklion for their support during my master studies.

Abstract

Transrectal ultrasound (TRUS)-guided brachytherapy is a treatment option for prostate cancer which involves the implantation of seeds into the prostate. Seed localization is important for the evaluation of implants' distribution, which will reveal any deviations from the prescribed dose .This report, describes a method of automatic seed detection using 3D ultrasound images, which could be performed by an image-guided brachytherapy robot during the intraoperative dosimetry procedure.

One dimensional Hough transform is applied to detect the trace of a seed, a bright 'tail' of pixels, in pre-scan converted ultrasound images. The purpose of the proposed method is to define seeds candidates of an ultrasound volume for further image processing. The experiments with P.V.C. phantom showed that the true positive rate for seed detection is 100%.

Key words: seed detection, prostate brachytherapy, intraoperative dosimetry, ultrasound imaging, Hough transform

Résumé

Curiethérapie échographie transrectale (TRUS)-guidée est une option de traitement pour le cancer de la prostate qui consiste à l'implantation de graines dans la prostate. La localisation des graines est importante pour l'évaluation de la distribution des implants, qui révélera les écarts par rapport à la dose prescrite. Le présent rapport, décrit une méthode de détection automatique des graines à partir d'images d'échographie 3D, ce qui pourrait être effectuée par un robot curiethérapie guidée par l'image au cours de la procédure de dosimétrie peropératoire.

Le transform unidimensionnel de Hough est appliquée pour détecter la trace d'une graine, une «brillante queue» de pixels, en images échographiques avant la conversion de scan. Le but de la méthode proposée consiste à définir les candidats graines d'un volume à ultrasons pour le traitement d'images supplémentaires. Les expériments avec P.V.C. fantôme ont montré que le taux de vrais correctes pour la détection de semences est de 100%.

Mots clés: la détection de graines, la curiethérapie de la prostate, la dosimétrie peropératoire, échographie, transform Hough

Περίληψη

Η βραχυθεραπεία υπό την καθοδήγηση διορθικών υπερήχων αποτελεί μια ελάχιστα παρεμβατική μέθοδο για τη θεραπεία του καρκίνου του προστάτου. Η ακτινοβολία εναποτίθεται στον προστάτη με την εμφύτευση ραδιενεργών κόκκων στον ιστό του αδένα. Ο εντοπισμός των κόκκων διαδραματίζει καθοριστικό ρόλο για την εκτίμηση της κατανομής τους (διεγχειρητική δοσιμετρία) και την απόκκλιση αυτής από την αρχικά ορισμένη δοσολογία της ακτινοβολίας. Η παρούσα εργασία περιγράφει μια τεχνική αυτόματης ανίχνευσης των ραδιενεργών κόκκων στο τρισδιάστατο υπερηχογράφημα του προστάτου και μπορεί να ενσωματωθεί σε ενα ρομποτικό σύστημα βραχυθεραπείας απεικονιστικά καθοδηγούμενο.

Κάθε ραδιενεργός κόκκος φέρει ένα ίχνος, μια «ουρά» φωτεινών pixel. Η αναγνώριση του ίχνους επιτυγχάνεται εφαρμόζοντας μονοδιάστατο μετασχηματισμό Hough για την εύρεση γραμμών σε εικόνες υπερήχων, που λαμβάνονται απο σάρωση κυκλικού τομέα (pre-scan converted images). Σκοπός της προτεινόμενης μεθόδου είναι να καθοριστούν τα σημεία της τρισδιάστατης εικόνας του προστάτου, που ειναι πιθανό να αντιστοιχούν σε ραδιενεργούς κόκκους. Απαιτείται περαιτέρω επεξεργασία της εικόνας για τον τελικό εντοπισμό των κόκκων. Πρώιμα αποτελέσματα απο τα πειράματα που πραγματοποιήθηκαν έδειξαν οτι ο συνδυασμός πολλαπλών προβολών του προστάτου απορρίπτει αρκετά απο τα σημεία που λανθασμένα αναγνώρισε ο Hough ως κόκκους. Για τη διενέργεια των πειραμάτων χρησιμοποιήθηκε ομοίωμα προστάτη κατασκευασμένο από P.V.C. Το ποσοστό των αληθώς θετικών αποτελεσμάτων (true positive rate) ηταν 100%.

Λέξεις κλειδιά: εντοπισμός κόκκων, βραχυθεραπεία προστάτου, διεγχειρητικη δοσιμετρία, απεικόνιση υπερήχου, μετασχηματισμός Hough

Summary

Brachytherapy has emerged as a potential treatment technique for patients with early stage prostate cancer, which provides an alternative to radical surgery or external beam radiation therapy. In this procedure, automatic seed detection is significant for the evaluation of intraoperative dosimetry and an efficient re-planning. Previous work was concentrated on seed localization in CT, fluoroscopic and ultrasound images producing encouraging results but clinically robust tracking and localization of the implanted seeds in ultrasound images is unavailable. In this report is proposed an algorithm that uses ultrasound images and performs one dimensional Hough transform for each intensity local maximum. The purpose of this technique is to define candidate seeds in ultrasound images, which will reveal the real seeds with further image processing. To verify the efficacy of the method, a P.V.C phantom was built to simulate the prostate.

Contents

1 Introduction

1.1 Image-guided therapy and medical robotics

Hippocrates (460-377 B.C) and Galen (131-201 A.D) were the first physicians to document their patient's process of healing to improve patient care. This completely changed how we viewed diseases. They were no longer some mysterious fatal force. The medical practice in ancient times was about gathering information and processing information. Since that time, the scientific community needed 19 centuries to incorporate the technological achievements in medical applications. Nevertheless, the last two decades there is an astonishing evolution in the medical field with the creation of robotic devices and complex imaging.

Image-guided therapy, a domain of computer-assisted surgery, allows us to see inside the body so that we can perform medical procedures with greater accuracy and using minimally invasive techniques. It can strongly benefit from using robotic devices in order to ameliorate the performance of the physicians. This technology is based on four principles:

- *Imaging*
- *Planning*
- *Registration*
- *Tracking and Navigation*

The advantages derived from the use of computer equipment in the operating rooms are numerous and diverse. Surgical procedures are accomplished at a higher level of speed and quality. The surgeons' fatigue level is reduced and they experience less of the tremors effect. A number of postoperative complications may be avoided and the hospitalization time may shorten. In some cases the patient is safe to go home right after the operation. An example is the Da Vinci system (Figure 1), with which it is possible to operate on the heart by making three or four small incisions in the chest, each only about 1 centimeter in length. Because the surgeon would make these smaller incisions instead of a single large opening in the chest, the patient would experience less pain, trauma and bleeding, leading to a faster recovery. Another great achievement of medical technology is the contribution to the treatment of prostate and breast cancer through brachytherapy. The rest of the report is going to describe the usefulness of prostate brachytherapy and how it can be improved through image-guided devices.

1.2 Brachytherapy

Brachytherapy is an advanced cancer treatment. Derived from ancient Greek words for short distance (brachy, βραχύς) and treatment (therapy, θεραπεία), it is sometimes called seed implantation and is used in the treatment of different kinds of cancer. Radioactive "seeds" are carefully placed in or close to the cancerous tissue,

giving a high radiation dose to the tumor while reducing the radiation exposure in the surrounding healthy area. Some of the diseases now treated with brachytherapy include prostate cancer, cervical cancer, endometrial cancer, and coronary artery disease. Brachytherapy has been proven to be very effective and safe, providing a good alternative to surgical removal of the prostate, breast, and cervix, while reducing the risk of certain long-term side effects.

Figure 1: Da Vinci system

1.2.1 Prostate brachytherapy

Prostate brachytherapy is a method of treating cancer that has not spread beyond the prostate gland. Using ultrasound image guidance (Figure 2), radioactive seeds are placed into the prostate via needles inserted through the perineum (skin just behind the scrotum).

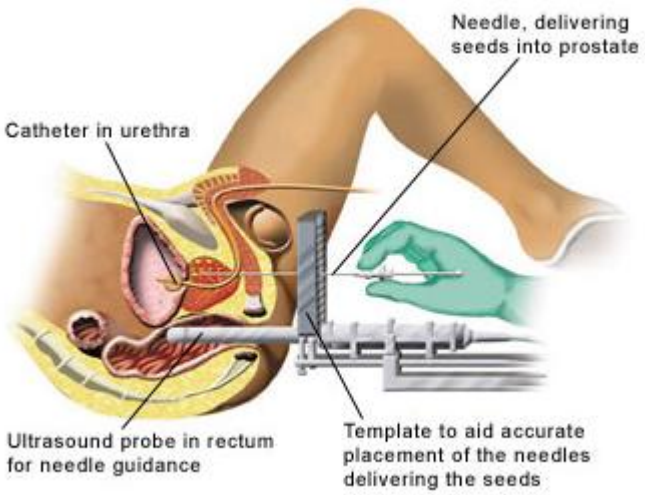

Figure 2:The surgeon inserts the implants under ultrasound guidance

In the treatment of prostate cancer, the radioactive seeds are about the size of a grain of rice (Figure 3), and give off radiation that travels only a few millimeters to kill

nearby cancer cells. The radioactivity of the seeds rapidly decays with time while the actual seeds permanently stay within the treatment area.

Figure 3: Radioactive seeds

During the Procedure:

The actual procedure takes approximately 2 hours. An ultrasound probe is inserted into the rectum, which will show the prostate gland on a television monitor, to aid the doctor in placement of the seeds. The first step in the brachytherapy procedure is the use of ultrasound to determine the position and the shape of the prostate (Figure 4) through the collection of a set of parallel 2D ultrasound images taken over the gland. Once the size of the patients prostate is figured out, the physician is able to proceed to dose pre-planning. By the help of specific software, he is able to calculate the distribution (Figure 5) of radioactive seeds that should be delivered into the prostate for the brachytherapy in order to give the planned dose whilst sparing organs at risks (urethra, rectum). This procedure is referred as dosimetry or dose planning.

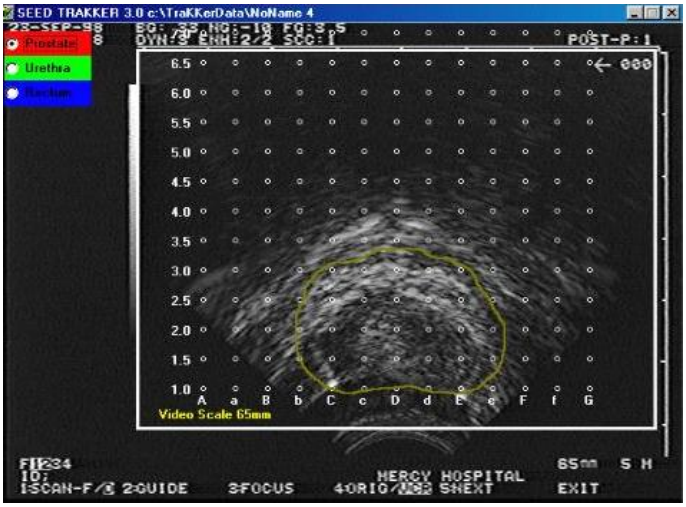

Figure 4: The yellow contour defines the prostate's shape

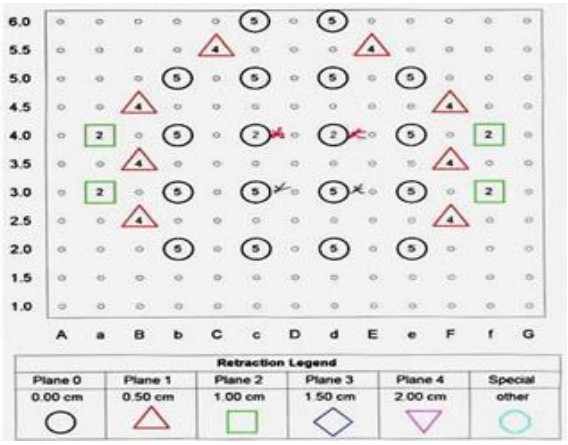

Figure 5: A special form that radiologists use to plan the dosimetry.

The seeds are then implanted into the prostate through very thin needles. The needles are guided by a fixed template (Figure 6) that corresponds to the grid (Figure 3) shown in the ultrasound image of the prostate. Depending on different variables (such as the size of the gland), between 50 and 100 seeds are used. The type of seeds also varies and may include Iodine-125, Palladium-103, and echnogenic Iodine-125 seeds. The needles are inserted into the skin between the scrotum and rectum and are guided under ultrasound control to the right place to most effectively treat the cancer.

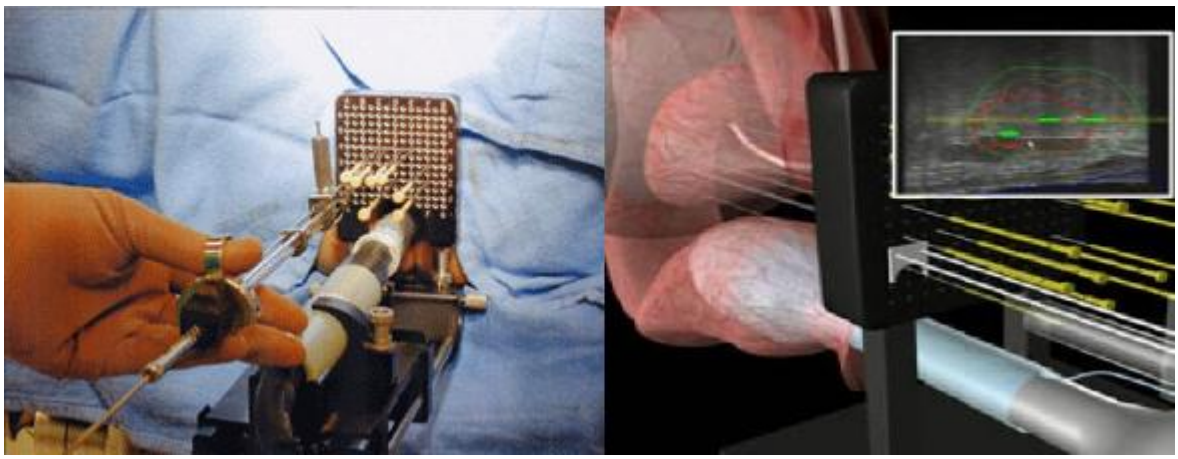

(a) (b)

Figure 6: (a) Needles are inserted through the perineal template at the periphery of the prostate, (b) An illustration of brachytherapy, showing needles that are used to implant the radioactive seeds into the prostate and the use of ultrasound to assess their location in real-time.

Post implantation:

One month after the implantation a fluoroscopic scan is performed (Figure 7) to enable physicians to estimate the position of each seed in the prostate. Fluoroscopy is a type of medical imaging that shows a continuous x-ray image on a monitor, much like an x-ray movie. This is necessary to determine that the prostate gland is receiving the proper amount of radiation throughout the entire gland. On rare occasions, it has been

necessary to give an additional amount of radiation with external radiation or another implant.

Figure 7: Fluoroscopy X-ray image of the prostate area

2 Intraoperative Dosimetry and Seed Detection

2.1 The importance of intraoperative dosimetry

Dosimetry in general is defined as the calculation of absorbed dose and its optimization in radiation therapy. In brachytherapy the intraoperative dosimetry is a crucial factor of the treatment planning. It is possible for the implantation evaluation to reveal underdosed areas of the prostate and unnecessarily irradiated healthy tissues. These inaccuracies have different reasons: the prostate moves and is deformed due to the ultrasound probe movements and to the insertion of needles; its volume is modified during the procedure because of bleeding; finally, the needles are deformed during insertion in the tissues. This postoperative impact could be prevented, if the physicians were provided with a real-time dosimetric feedback during prostate brachytherapy. The need for intraoperative dosimetry was intrigued by the advent of frameworks that could manage the optimization of both seed placement and dose distribution [1, 2, 3, 4, 5] in the treatment planning. In [6] the authors made a statistic observation that was derived from patients' data and emphasizes the importance of having the ability to re-adjust the distribution of implants. Figure 8 illustrates the magnitude of the problem by comparing for a random group of 17 patients, the percentage urethral volume covered by 150% of the prescription dose (planned or assessed at post-implant evaluation) and also 200% of the prescribed dose (post implant evaluation; the planned percentage volume was always zero). An efficient method of seed localization could be a reliable tool in the hands physicians, as they would be able to measure the distribution of the radioactive implants and schedule a real-time re-planning.

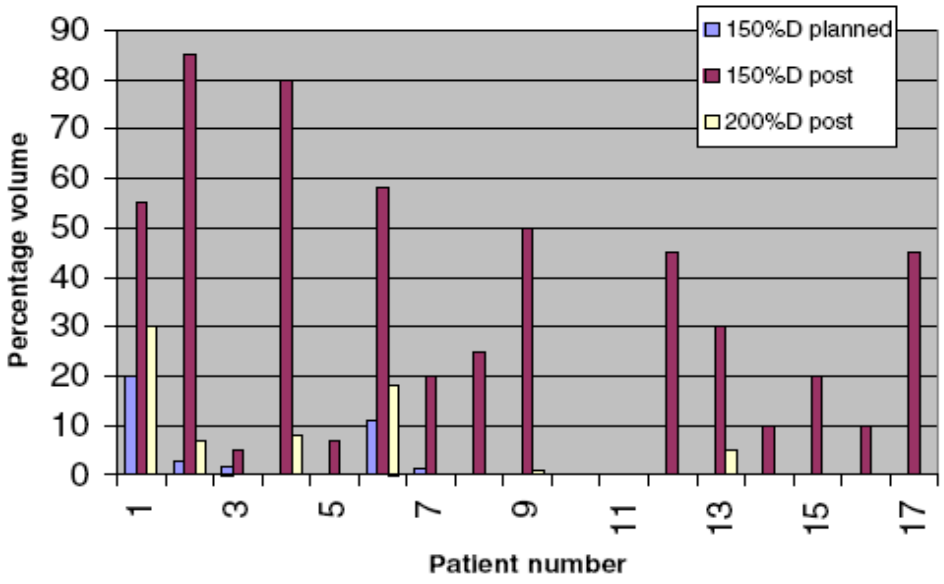

Figure 8: Percentage urethral volume covered by the stated percentage of the prescription dose.

3 Background and Related Work

3.1 Imaging modalities in seed detection

The last decade, seed detection has been a challenging research issue. The reports that have been published perform seed localization on CT (computed tomography), fluoroscopic or ultrasound images. A CT scan is a 3D imaging method that uses x-rays to create cross-sectional pictures of the body. A fluoroscopic image is also produced from x-rays and it can be acquired in real-time but it is a projective image. An ultrasound image involves sending out high-frequency sound waves. These waves reflect off body structures and the strength of these reflections is depicted in the image. The advantage of CT and fluoroscopy is that they provide high contrast images which assure a clear view of the seeds, although the boundaries of soft tissue, like prostate and urethra, are shown poorly. Unfortunately, the use of these imaging modes carries some severe side effects due to the patient‘s exposure to radiation. On the other hand the ultrasound modality (2D or 3D) is noisy and not so rich in contrast information, however, the prostate is much more visible on ultrasound than on X-ray modalities. MRI (magnetic resonance imaging) is based on the principles of nuclear magnetic resonance (NMR), a spectroscopy technique used by scientists to obtain microscopic chemical and physical information about molecules. MRI has several potential advantages over fluoroscopy as it does not expose the patient to ionizing radiation, it allows 2D and 3D imaging with arbitrary slice orientation and thickness and can obtain not only anatomical but also physiological information. Nevertheless it suffers from the slicing effect, unlike ultrasound images.

3.2 Research on seed detection using CT or fluoroscopic

During the past years, several approaches were developed for localization of the seeds in CT or fluoroscopic images. Teodor et al [6] performed studies on intra-operative dynamic dosimetry. They determined the number of seeds within a cluster by measuring the characteristics of each cluster of seeds and processing the morphological differentiation using the fluoroscopic image of the prostate which was acquired in patient’s visit before the brachytherapy operation .They also discussed the localization problem of hidden seeds (partial or total area of a seed is behind another seed). Methods similar to the previous cannot be reliable, considering the fact that the prostate is not in the same position as during the seed implantation. In addition, the incapability of these images to outline the prostate‘s boundaries increases the possibility of errors [7, 8]. In some other reports [6, 9, 10] a reconstruction model of 3D coordinates from projections was presented. In the case of overlapped seeds which occurs very often in those projection images, correction algorithms had to be used, which proved out to be complicated [10]. The authors in [17] contributed to 3D localization of implanted radioactive seeds from the aspect of algorithmic information theory. They introduced an

algorithm which could find an optimal solution from multiple projection images with hidden seeds and be performed in polynomial time.

3.3 Research on seed detection using MRI images

MR modality is widely used in image-guided brachytherapy robots. It has been investigated profoundly in the area of image registration and prostate segmentation. This prior knowledge of MRI capabilities attracted the interest of researchers working on the problem of seed detection. An MR image is better in visualizing the prostate gland but poor in localizing the seeds. In [18] the authors used an optimized MR scanning sequence to identify prostate implants. Inspired by this effort Lee et al [19] proposed a semi automatic seed extraction algorithm. The algorithm determines x, y and z coordinates of the seed centers from MR images and registers their locations to the patient anatomy.

3.4 Research on seed detection using Ultrasound images

In [11, 12, 13] the authors presented significant work in seed detection under 3D ultrasound guidance. Their goal was to build an efficient framework for transperineal prostate brachytherapy. A dynamic intraoperative procedure, in which all steps are performed in one session, including planning, monitoring of the prostate changes, dynamic re-planning, optimal needle insertion and automatic seed localization in US images, that would help solving some of the problems with current prostate brachytherapy [6]. Especially for seed detection, the algorithm that they developed involves five steps:

- 3D needle segmentation.
- Volume cropping along the detected needle trajectory.
- Non-seed structure removal based on tri-bar model projection.
- Seed candidate recognition using 3D line segment detection.
- Localization of the seed positions

This approach is based on the knowledge of needle ‘s position, which is located by performing 3D needle segmentation.The authors are making the logical assumption that a seed will be placed close to the needle and inside the boundaries of rectangular area along the needle trajectory. These regions may contain bright spots, which belong either to tissues or seeds. In order to distinguish the spots, they used a rigid, tri-bar model. Finally the seed candidate recognition was accomplished in 3D US frame difference image, where each frame is subtracted from the previous frame and each surface produces two parallel lines, the top and bottom part of the seed. A threshold on the number of 3D line segments was the criterion to decide about the existence of a seed. Finally they localize the seed‘s center. For the experiments they used agar and turkey/chicken phantoms (Figure 9).

Wen and Salcudean [20] proposed a differed approach. They proposed a seed detection method using 3D ultrasound. Instead of using conventional B-mode images, reflected power images are computed from ultrasound radio-frequency signals and then used to reconstruct a 3D volume. Finally implanted seeds are segmented in local 3D search spaces.

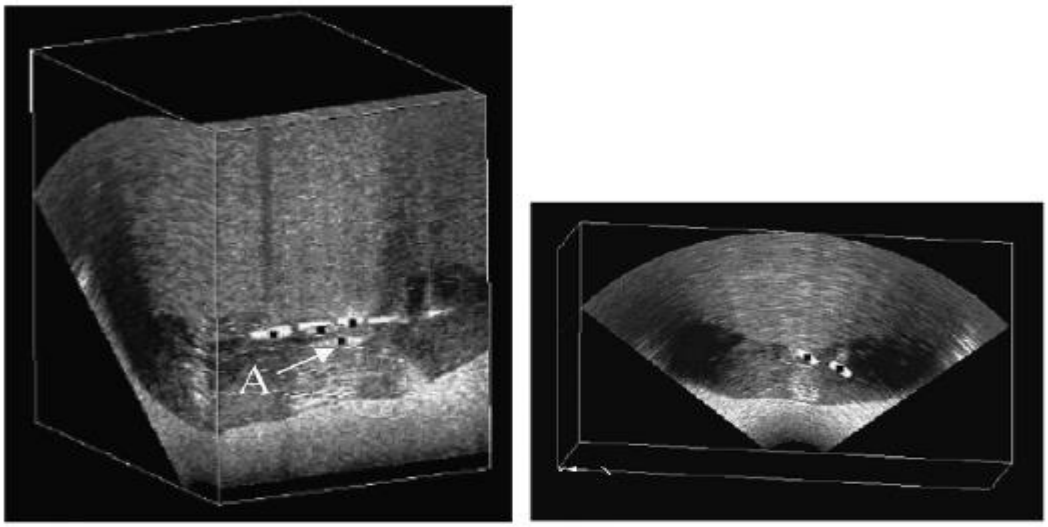

Figure 9: Segmented seeds in a chicken phantom. The white spots are the actual seeds while the black spots are the segmented seeds. There are four seeds in the first image but the fourth seed indicated by an arrow is a false segmentation as designated by ‘‘A’’ on the second line; the two seeds in the second image were segmented correct.

3.5 A strategy for automatic seed detection

The purpose of the current research is to investigate different methods of image processing and eventually to determine an efficient framework of automatic seed detection. The strategy that is proposed in this report evolves in three stages:

- *Acquisition of 3D TRUS volume after implantation of a line of seeds:* The acquisition of 3D TRUS volume (both pre-scan and scan converted) after each implantation assures that in vivo dosimetry is updated during the brachytherapy.

- *Detection of ‘candidate seeds’ in pre-scan converted images which are not biased by interpolation artifacts:* The use of pre-scan images has the advantage of not being biased by interpolation artifacts. The scan-converted images are produced from interpolating pre-scan converted ones. At this step some seed candidates are going to be detected from their characteristic trace, a bright tail. One-dimensional Hough transform on local intensity maxima of TRUS images is the algorithm that is proposed to perform this task.

- *Final detection in registered scan-converted images:* The pre-scan converted images are transformed to scan converted. Thus the seed candidates are identified also

in scan converted images. It is expected that the knowledge of candidates in combination with the foreground recognition will lead to final definition of the seeds. The foreground will include all the bright objects of the image and their recognition is proposed to be delivered by a background subtraction approach where an image without seeds is subtracted from the corresponding with seeds.

4 Proposed Algorithm: 1D Hough Transform on local intensity maxima of TRUS images

4.1 Hough Transform in General

The Hough transform is a feature extraction method for locating patterns in images. The purpose of this technique is to find curves that can be parameterized like straight lines, polynomials, circles etc. It can be used in 1D, 2D, 3D space or even in higher dimensions.

Curve	***Classical HT***	***Generalized HT***	***Dimensional Space***
Line	$y = \alpha x$	$y = -x * \operatorname{atan}(\theta)$	1D
	$y = \alpha * x + \beta$	$\rho = x * \cos(\theta) + y * \sin(\theta)$	2D
Circle	$\rho^2 = (x-\alpha)^2 + (x-\beta)^2$	$x = \alpha + \rho * \cos(\theta)$	2D
		$y = \beta + \rho * \sin(\theta)$	
Ellipse	$((x-h) / \alpha)^2 + ((y-k) / \beta)^2 = 1$	$x = \alpha_0 + \alpha_x * \sin(\theta) + \beta_x * \cos(\theta)$	2D
		$y = \beta_0 + \alpha_y * \sin(\theta) + \beta_y * \cos(\theta)$	
Planar	$\alpha * x + \beta * y + \gamma * z + 1 = 0$	$\rho = x * \cos(\theta) + y * \cos(\varphi) + \gamma * \cos(\omega)$	3D

Table 1: Examples of Hough Transform

In 1959 [14] classical Hough transform was introduced by P.V.C. Hough. It was based on using slope-intercept parameters (Table 1, classical HT). In 1972, Duda and Hart [15] mentioned an important progress in the algorithm. They proposed the use of polar coordinates (Table 1, generalized HT) for representing the curves. This suggestion implies the conversion of Cartesian coordinates (x, y) into polar coordinates (Figure 10). Their contribution was useful as it could overcome crucial limitations of the initial algorithm, such as the case of horizontal or vertical slope (x=0 or y=0). The Hough transform works by letting each feature point (x, y) vote in (ρ, θ) space for each possible line passing through it. These votes are summed in an accumulator. Finally a threshold for the bins' values H(θ,ρ) is used.

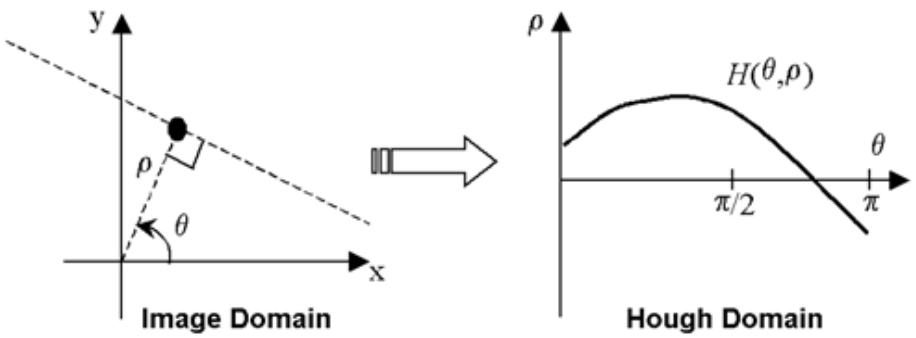

Figure 10: The first image (Image Domain) shows a parametric line in Cartesian coordinates and its Hough transform is shown at the second image (Hough Domain) .

One of the most useful properties of Hough transform is its tolerance of gaps in feature boundary descriptions and the fact that is relatively unaffected by image noise unlike edge detectors. An example is shown in Figure 11.

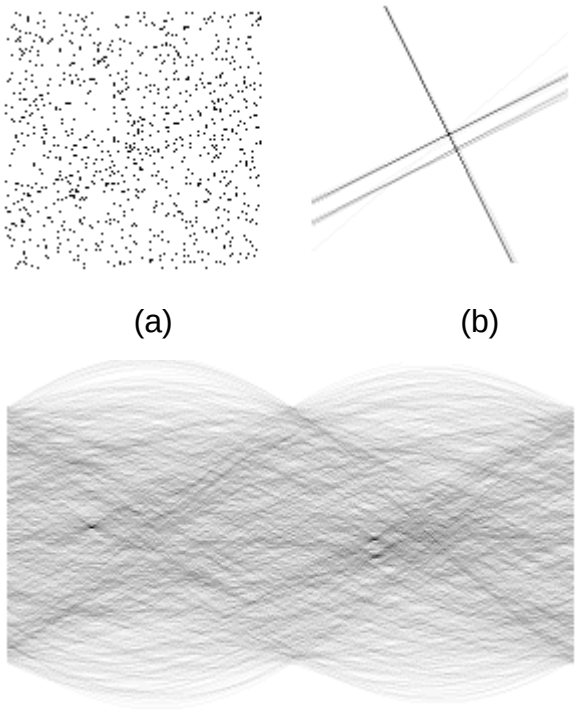

(a) (b)

(c)

Figure 11: (a) A random image with noise and lines, (b) The lines are the Hough transform backprojection of image (a), (c) The Hough transform of (a).The three bins that that seem more black than the others correspond to the lines in (b).

4.2 1D Hough Transform on local intensity maxima of TRUS images

As reviewed in section 3, several methods have been published for seed localization in prostate brachytherapy. Their goal was either to distinguish the shape of a seed or to reconstruct its coordinates. The proposed algorithm attempts to locate the trace of the seed instead of the implant's shape. It is easier to analyze this area, since it always lies in the scanline. For this purpose the pre-scan converted US images were studied. At this point, it would be helpful to mention that scan-converted images are produced as an interpolation result of the pre-scan ones, which implies some loss of information (Figure12a, 12b).

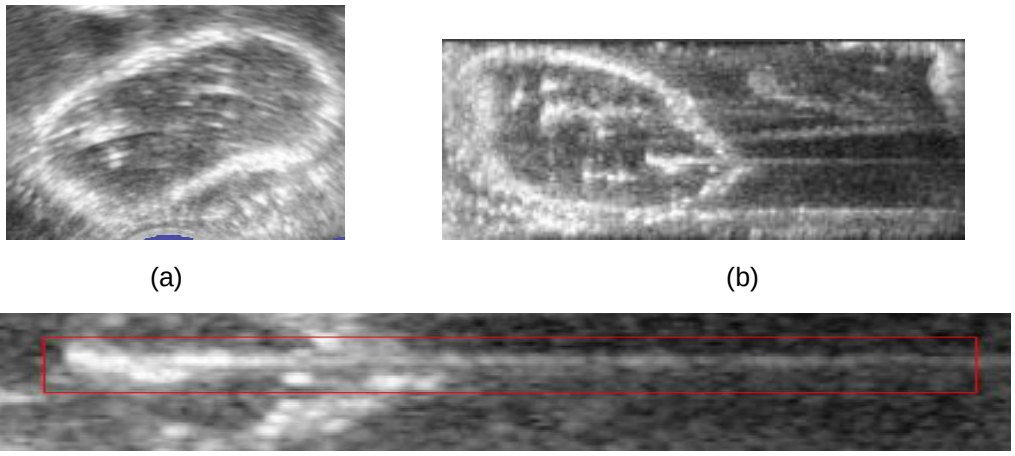

(a) (b)

(c)

Figure: (a) Scan converted image, (b) Pre- scan converted image, (c) Bright tail of a seed

The implant is metallic, which according to acoustics principles means that the transducer will receive a strong reflected echo. This echo is interpreted as local intensity maximum of the pre-scan US image. The algorithm assumes that all intensity maxima are elements of interest. It was observed that the seed is followed by a bright tail (Figure 12c). The next step is to check which elements correspond to a trace. More precisely it must be investigated if there are any collinear bright pixels at the right side of each element. The 1D Hough transform applied for detecting lines is a suitable technique to accomplish this task. For the purposes of executing 1D Hough transform, it needs to convert Cartesian coordinates (x, y) into polar coordinates (θ, N) where N is the normalized intensity value of pixel (x, y) and θ is the angle between the axis and the line connecting the pixel (x, y) to the origin .

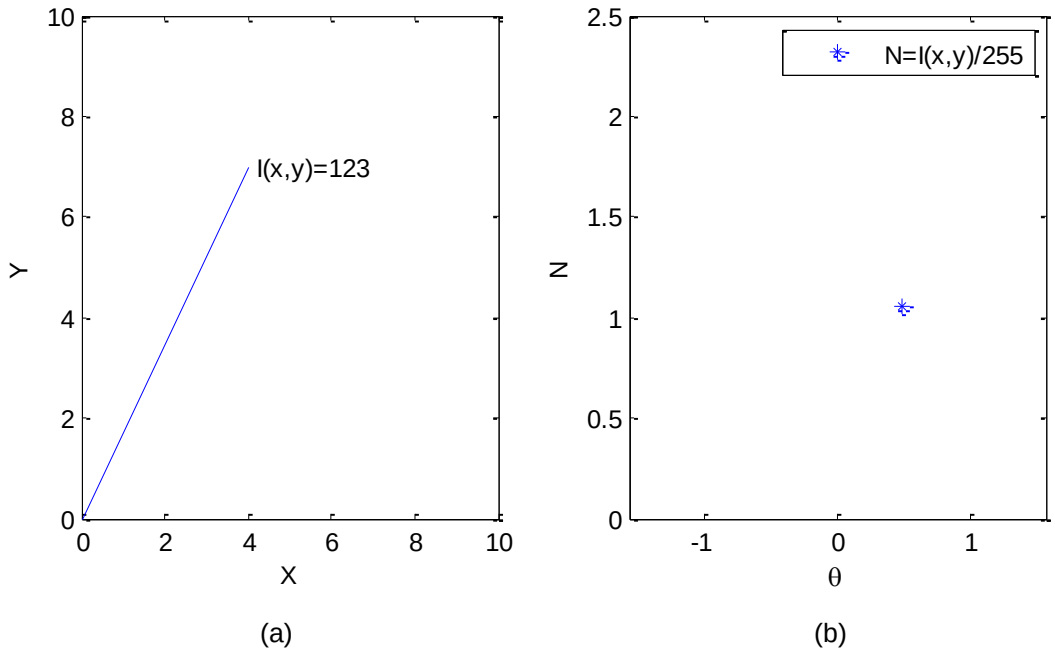

Figure 13: (a) Cartesian system, (b) Polar system

In Figure 13, is shown the data in Cartesian space and in polar space. Using the formula y=-x *atan(θ) the transform corresponds a line to a point. Another crucial aspect of the algorithm is the definition of the search space where Hough transform is going to be applied. The rectangular area (Figure 14b) at the right of the element is cropped in a way that is possible to maintain the majority of tail's bright pixels. It is chosen a radius that outlines a hemisphere where the bright tail is enclosed (Figure 14b). The radius varies as it depends on the attenuation ratio how rapidly the echo of the seed fades out. The next step is to build the Hough accumulator. The accumulator is an array of 181 equally spaced bins. Each bin corresponds to angles in the range [φ-1, φ) where $\varphi \in \mathbb{Z}$ and φ∈[-89,90]. The accumulator is initialized to zeros. For each pair (θ, N) the bin that contains θ is calculated and the value N is added to it. When all pairs (θ, N) of the hemisphere have contributed to the accumulator a double criterion is applied. If the 91st bin, which contains angles in the range of [0, 1) degrees, is the maximum of the accumulator and above a threshold, then the algorithm decides that the element is a candidate seed. The threshold should assure that at least the 70% of the N values added to the specific bin correspond to bright pixels (pixels of high intensity value) (Table 2).

(a)

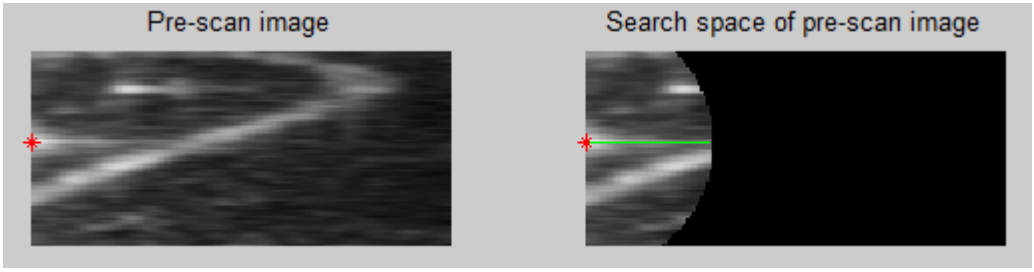

(b)

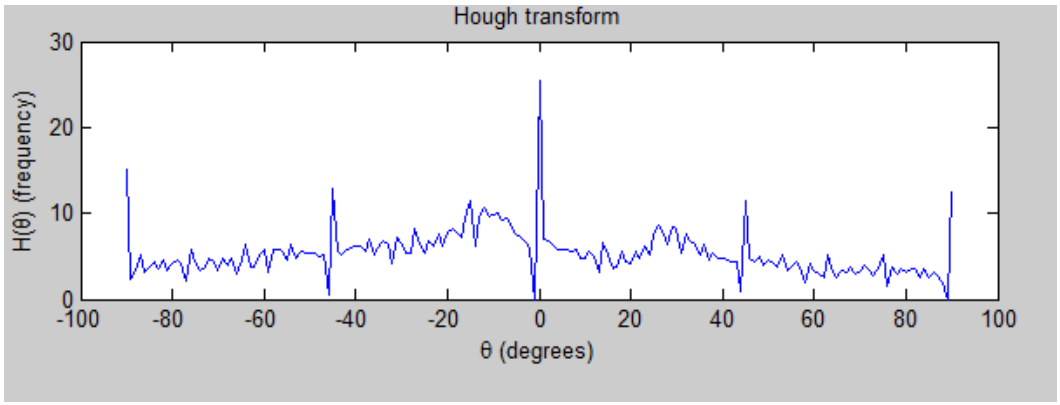

(c)

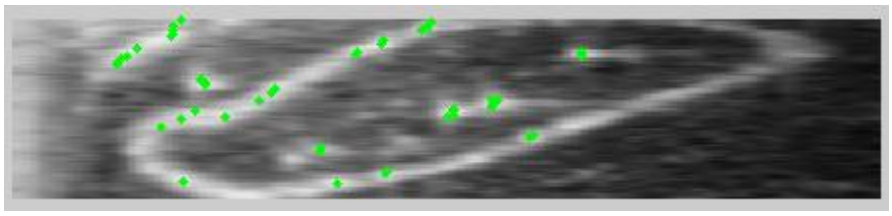

(d)

Figure 14: (a) Pre-scan converted image, (b) Results of performing 1D Hough transform on a local intensity maximum. The red point in the first two images is the local intensity maximum that is checked if it could be long to a seed. The last graph shows the 1D Hough transform. It is obvious that the bin [0,1) degrees is described by the maximum value of the accumulator. (c) The green points are the candidate seeds that have been detected after performing the 1D Hough on all local intensity maxima.

element:= element of interest

R: = radius of hemisphere, I: = intensity image

HoughTransform(element,R,I)

{ (a, b): = coordinates of the element

#SA is the search area of Hough and is defined as a hemisphere

SA: = {(x, y): $R^2=(x - a)^2 + (y - b)^2$ }

bin:= array of equally spaced 181 containers that partition angles between -90 and 90 degrees

accumulator:= array of size 181

For each (x, y) in SA

Calculate angle θ= atan(x, y)

Calculate angle N= I(x,y)/255

accumulator(bin(θ)) += accumulator(bin(θ))

end

bin(91) corresponds to the anpartition [0,1)

threshold= 0.7*R

if accumulator(bin(91)) is the maximum and bigger than threshold

the element is a seed candidate

else

the element is a not a seed candidate

end

end }

Table 2

4.3 Materials

A 3D TRUS transducer has been used to acquire the US volume of prostate phantom. A PVC seed phantom was conceived for a preliminary study (Figure). The interior of the phantom is non echogenic but there is higher echogenicity in the exterior layer. Ten non radioactive seeds were placed inside manually and are distributed in 3 levels, 30% of them at the top of the phantom, 40% at the middle and 30% at the bottom. They were oriented in random angles through manual insertion.

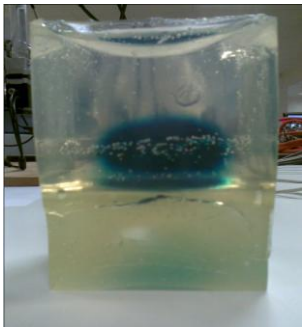

Figure 10 : PVC seed phantom

Figure 11: 3D TRUS transducer

5 Algorithm ‘s Results and Conclusions

5.1 Algorithm ‘s Results and Conclusions

The results of the algorithm were quite encouraging. The algorithm was verified in 200 frames acquired from a TRUS volume of the phantom described in section 4. From a set of 300.000 pixels, approximately 3500 pixels are considered to be seed candidates. The 70% of them are located on or outside the boundaries. All the seeds were identified amongst the candidates. A novelty method that could reduce more the candidates and exclude the outliers is the steering of transducer’s beams. Some preliminary experiments demonstrate that it could be effective. The steering is the rotation of the beams to an angle α., according to the geometry of the transducer (Figure 15).

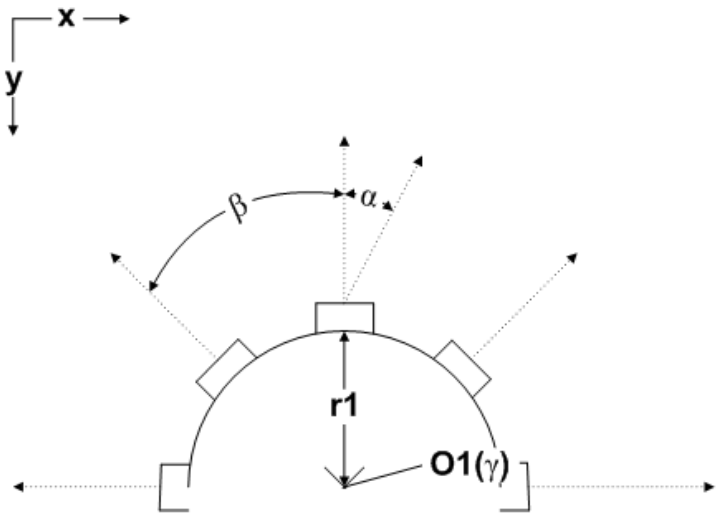

Figure 15 : Ultrasound Geometry

The purpose of changing the beams’ angle is to acquire ultrasound volumes from different views and project the seed candidates at the same image. In Figure 16 is shown an example where 1D Hough Transform on local intensity maxima was used to find seed candidates in a volume acquired from angle α=0 and in another volume where the angle was α=5 degrees. In the second image are shown all the candidates from the two different views projected in the image acquired from an angle of 0 degrees and in the third are shown the final candidates.

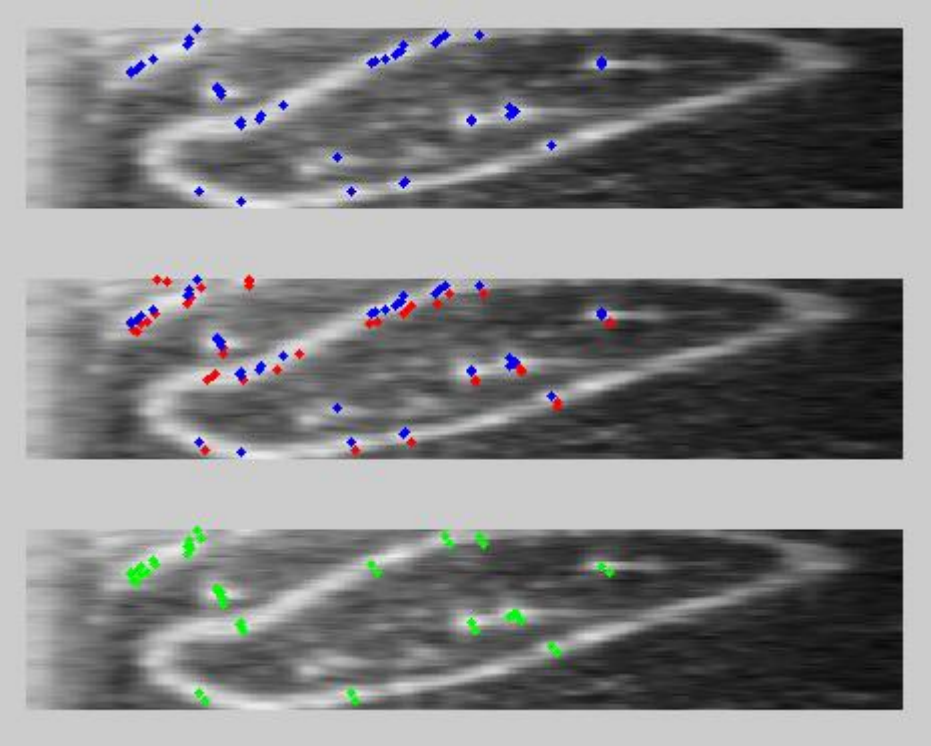

Figure 16: Projection of seed candidates

The process described before was implemented in 2 sets of 200 frames acquired from an angle 0 and 5 degrees respectively. It was impressive that taking into consideration only two projections was enough to reduce the candidates from approximately 3500 to 2200.

A major problem that was encountered during the research was the distortion of the bright tail due to the artifacts created by the outer layer of the phantom. It was hard to model it and remove as it could influence the attenuation of the bright tail in different positions and ways. This observation is obvious in the intensity profiles of the seeds' bright tails (Figure 17-23). Clinical data are required for the appropriate evaluation of the algorithm since the reflections from the outer layer and similar calcifications like bubbles in the phantom do not represent realistically the prostate.

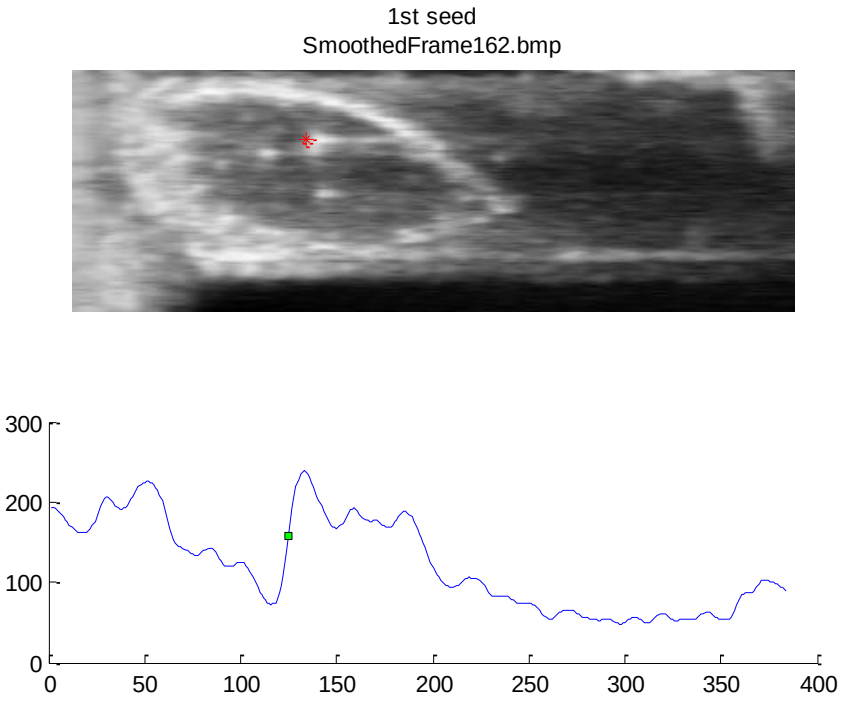

Figure 17: Pre-scan converted image and the intensity profile of the scanline where the seed (red point) is located

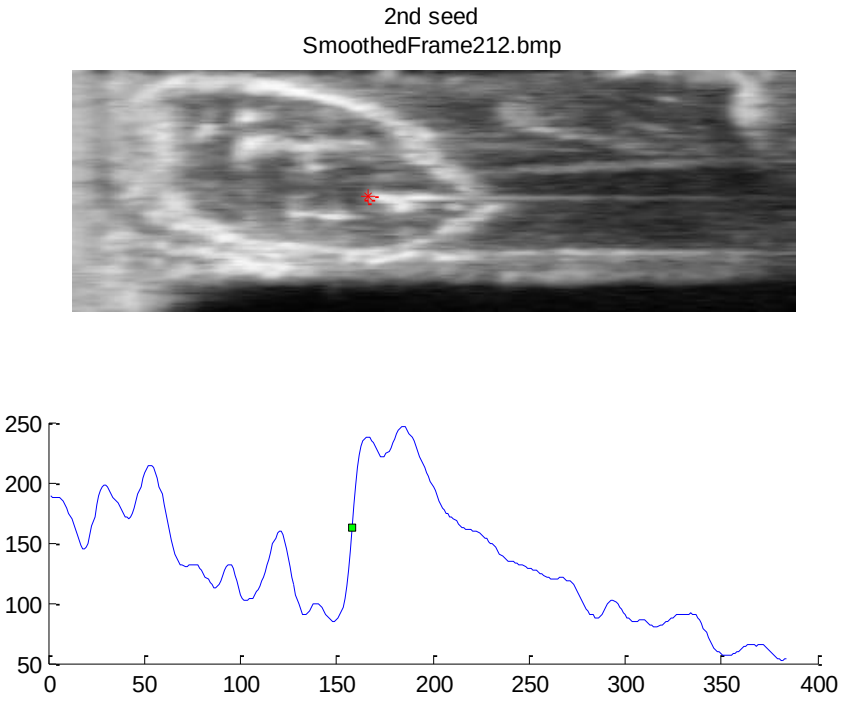

Figure 18: Pre-scan converted image and the intensity profile of the scanline where the seed (red point) is located

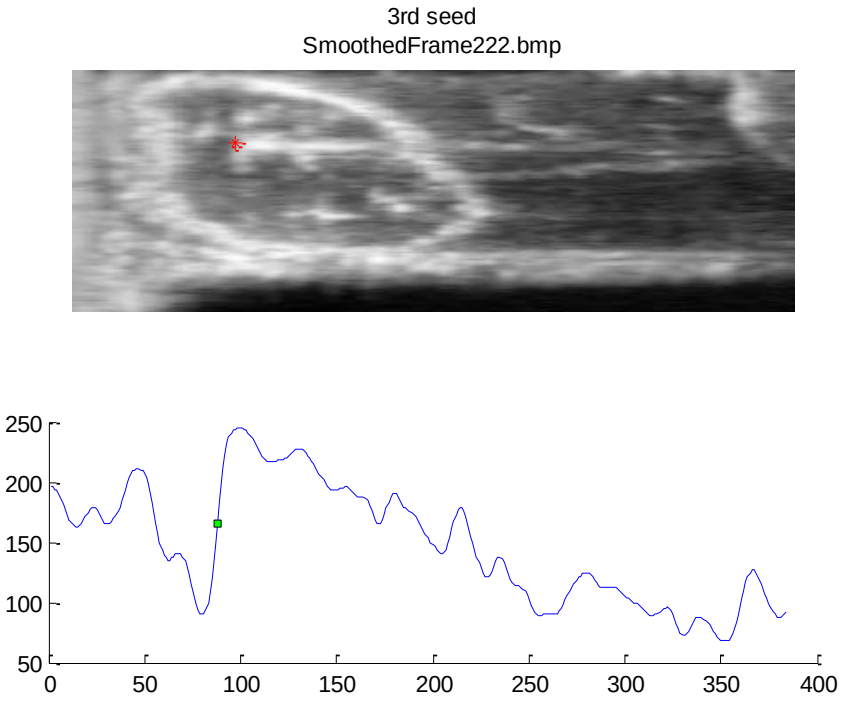

Figure 19: Pre-scan converted image and the intensity profile of the scanline where the seed (red point) is located

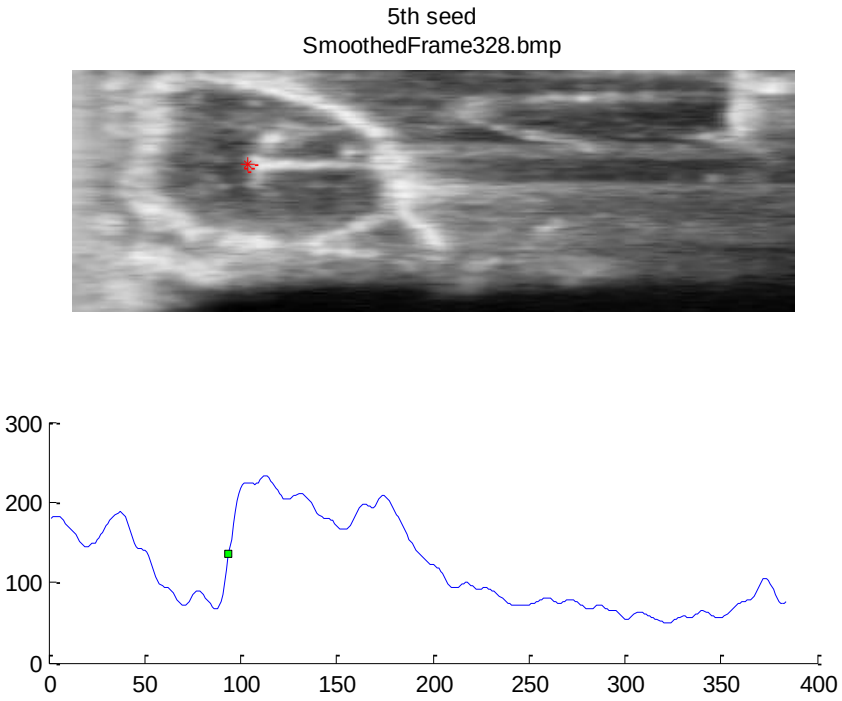

Figure 20: Pre-scan converted image and the intensity profile of the scanline where the seed (red point) is located

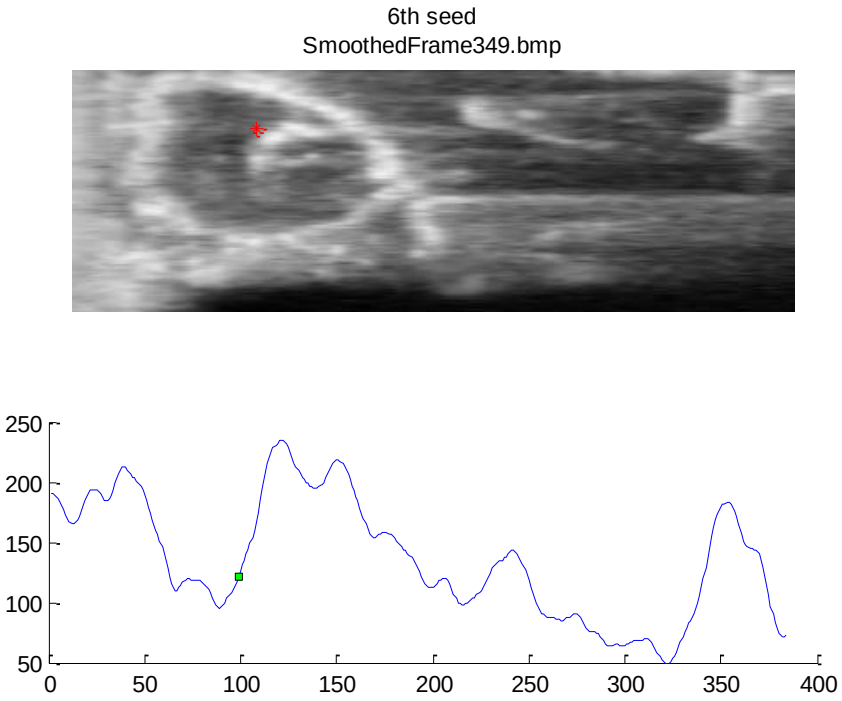

Figure 21: Pre-scan converted image and the intensity profile of the scanline where the seed (red point) is located

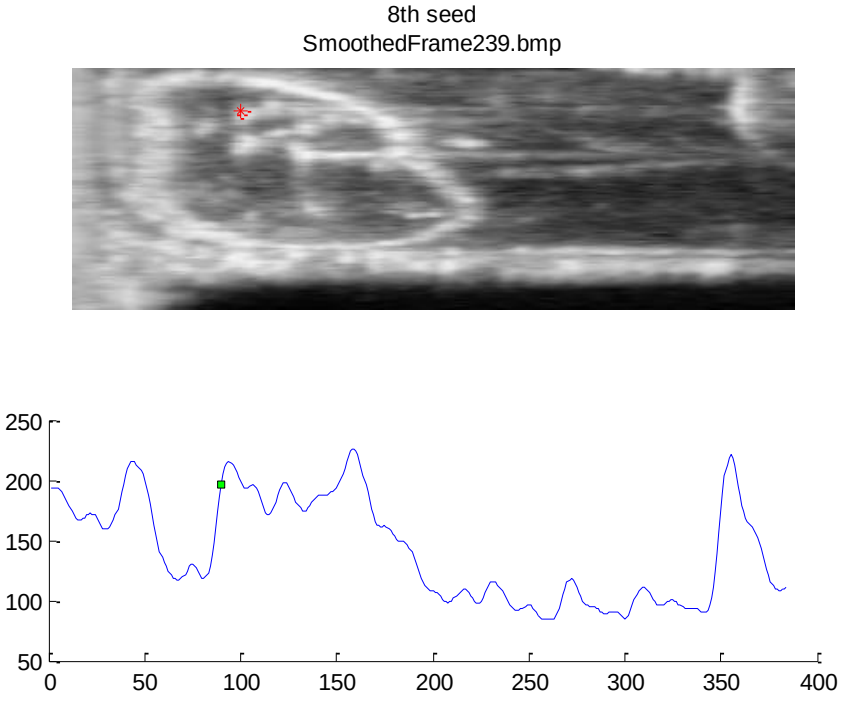

Figure 22: Pre-scan converted image and the intensity profile of the scanline where the seed (red point) is located

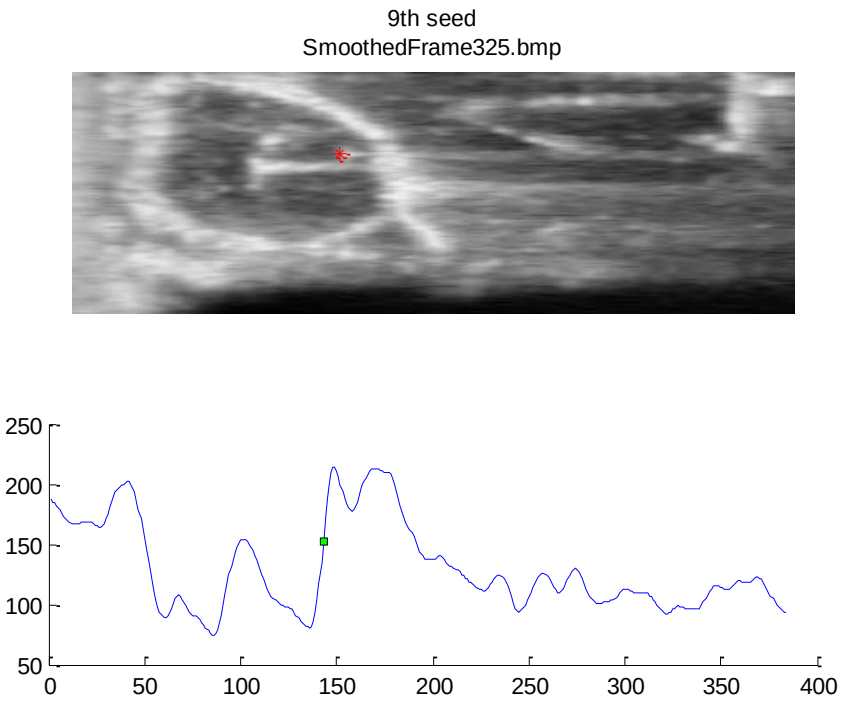

Figure 23: Pre-scan converted image and the intensity profile of the scanline where the seed (red point) is located

6 A Review on Other Methods

6.1 Background modeling

Another approach that was studied was the definition of a pattern that corresponds to a scanline with seed. The artifacts that are created from the boundaries of the phantom and from other seeds, are distorting the seed‘s attenuation ratio. This fact was a severe obstacle for creating a pattern for the seed.

The background model of a seed scanline was computed by using the 3D structure of the ultrasound volume. A square with an edge of 12 pixels was used to define which scan lines will contribute to the background. The centre of the square lies on the seed‘s scanline and outlines in the z-y plane of the ultrasound volume which scanlines will build the background model. This model is defined as the average intensity profile of the scanlines that are traversing the margins of the square. The next step is to subtract the background model from the seed scanline (Figure 24-27). The purpose of performing the background modeling was to clarify the seed scanline by removing the artifacts mentioned previously. This approach fails in cases where the seed is hidden or close to phantom ‘s boundaries, as the part o the scanline that characterizes the seed resembles to the computed background model (Figure 26).

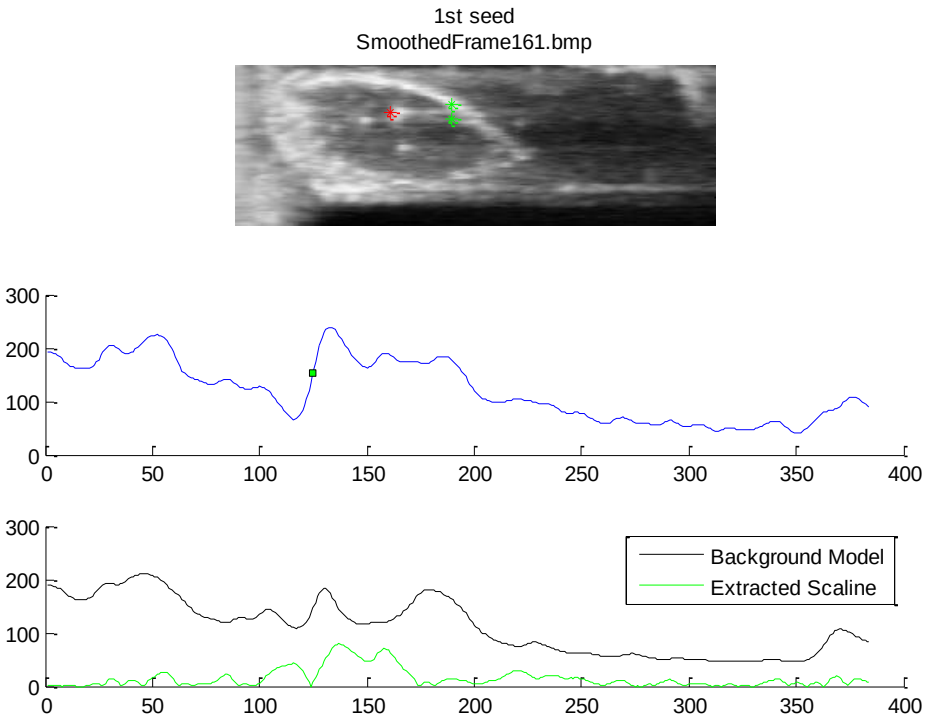

Figure 24: In the first image is shown the phantom ‘s image in x-z plane. The red point is the seed and the green point are the square‘s margins The first graph shows the seed’s scaline. The second graph shows the background model and the extracted scaline after the subtraction.

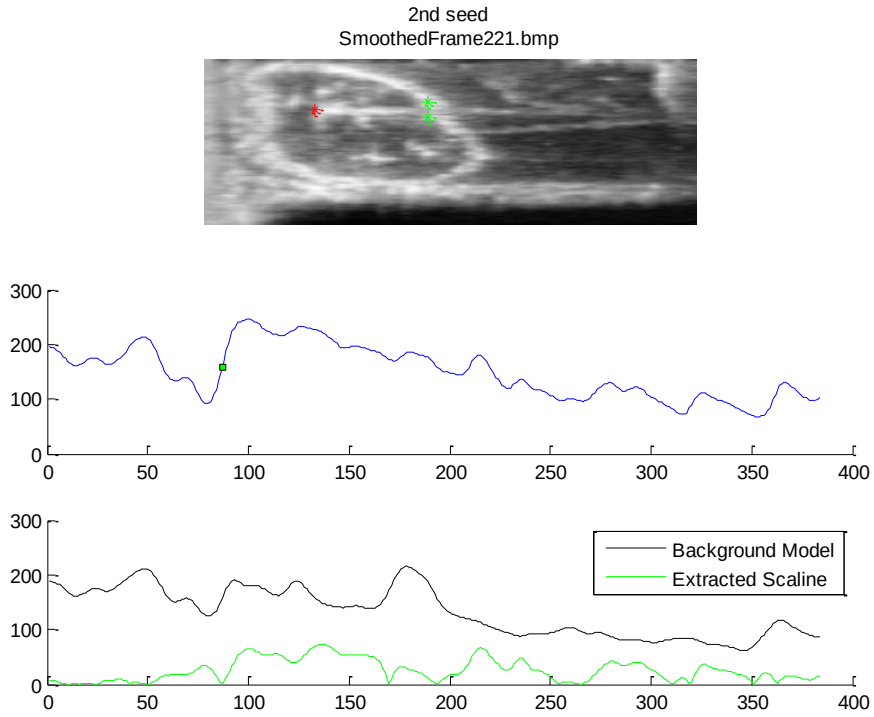

Figure 35: In the first image is shown the phantom ‘s image in x-z plane. The red point is the seed and the green point are the square‘s margins The first graph shows the seed’s scaline. The second graph shows the background model and the extracted scaline after the subtraction.

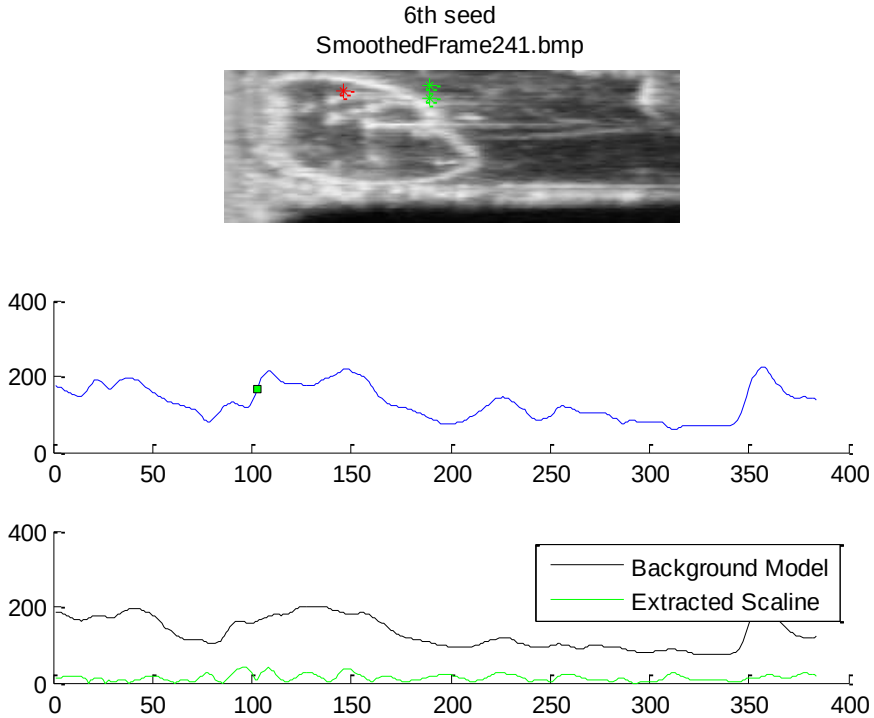

Figure 46: In the first image is shown the phantom ‘s image in x-z plane. The red point is the seed and the green point are the square‘s margins The first graph shows the seed’s scaline. The second graph shows the background model and the extracted scaline after the subtraction.

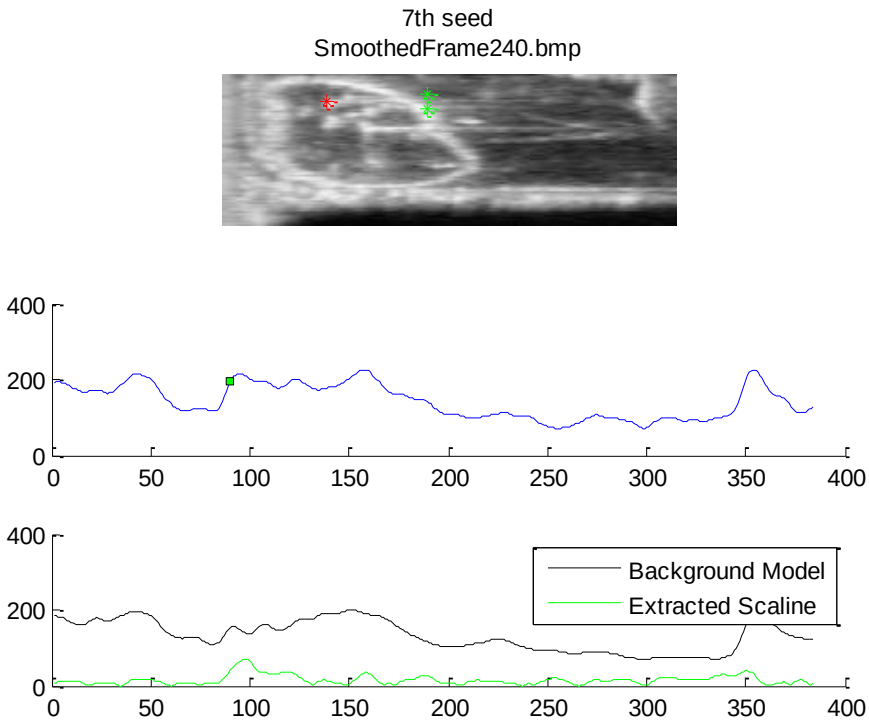

Figure 57: In the first image is shown the phantom ‘s image in x-z plane. The red point is the seed and the green point are the square‘s margins The first graph shows the seed’s scaline. The second graph shows the background model and the extracted scaline after the subtraction.

7 Future Work

This work proposes an algorithm that is based on the implementation of 1D Hough and detects seeds candidates by searching for their trace. Is important to emphasize that this approach is tolerant in noise and manages to overcome the artifacts from hidden seeds and phantom‘s boundaries that distort the seed‘s trace. Future developments of this technique concern the optimization of the radius, that defines the search space where 1D Hough transform is performed, and the research on the steering potentials to reduce the candidates. The experiments encourage further work on clinical data to evaluate the efficacy of the proposed strategy on seed detection.

Bibliography

1. **Lee, E., K.; Zaider, M.** *On the determination of an effective planning volume for permanent prostate implants.* s.l. : Int. J. Radiat. Oncol. Biol. Phys., 2001, Vol. 49, pp. 1197-206.

2. **Lee, E, K; Gallagher, R, J; Zaider, M.** *Planning implants of radionuclides for the treatement of prostate cancer:an application of mixed integer programming Optima.* s.l. : feature article, 1999b, Vol. 61, pp. 1-10.

3. **Zaider, M.; Zelefsky, M., J.; Lee, E., K.; Zakian, K., L.; Amols, H., I.; Dyke, J.; Cohen, G.; Hu, Y.; Endi, A., K.; Chui, C.; Koutcher, J., A.** *Treatment plannig for prostate implants using magnetic-resonance spectroscopy imaging.* s.l. : Int. J. Radiat. Oncol. Biol. Rhys, 2000, Vol. 47, pp. 1085-96.

4. **Lee, E., K.; Gallagher, R., J.; Zaider, M.** *Treatment planning for brachytherapy:An integer programming model,two computational approaches and experimentswith permanent prostate implant planning.* s.l. : Phys. Med. Biol, 1999a, 44, pp. 145-65.

5. **Silvern, D.; Lee, E., K.; Gallagher, R., J.; Stabile, L., G.; Ennis, R., D.; Moorthy, C., R.; Zaider, M.** *Treatment planning for permanent prostate implants: genetic algorithm versus integer programming.* s.l. : Med. Biol. Eng. Comput., 1997, Vol. 35, 2.

6. **Todor, D., A., et al.** Intraoperative dynamic dosimetry for prostate. s.l. : Phys. Med. Biol., 2003, Vol. 48, pp. 1153-1170.

7. **Roach, M.; Faillaceakazawa, P.; Malfatti, C.; Holland J.; Hricak, H.** *Prostate volume defined by magnatic resonance imaging and computerized tomographic scans for three-dimensional conformal radiotherapy.* s.l. : Int. J. Radiat. Oncol. Biol. Phys., 1997, Vol. 35, pp. 1011-1018.

8. **Rahmouni, A.; Yang, A.; Tempany, C., M.; Frenkel, T.; Epstein, J.; Walsh, P.; Leicher, P., K.; Ricci, C.; Zerbouni, E.** *Accuracy of in-vivo assessment of prostatic volume by MRI and transpectral ultrasonography.* s.l. : J. Comput. Assist. Tomogr., 1992, Vol. 16, pp. 935-940.

9. **Tubic, D.; Zaccarin, A.; Pouliot, J.; Beaulieu, L.** *Automated Sedd Detection and Tree-Dimensional Reconstruction. I. Seed localization from fluoroscopic images or radiographs.* s.l. : Medical Physics, 2001, Vol. 28, 11, pp. 2265-2271.

10. **Su, Y., et al.** *Prostate brachytherapy seed localization by analysis of multiple projections:Identifying and adressing the seed overlap problem.* s.l. : Medical Physics, 2004, Vol. 31, pp. 1277-1287.

11. **Wei, Z.; Ding, M.; Downey, D.; Fenster, A.** 3D TRUS Guided Robot Assisted Prostate Brachytherapy. 2005.

12. **Ding, M.; Wei, Z.; Gardi, L.; Downey, D.; Fenster, A.** *Needle and seed segmantation in intra-operative 3D ultrasound-guided prostate brachytherapy.* 2006.

13. **Wei, Z.; Gardi, L. Ding, M.; Downey, D.; Fenster, A.** *Segmentation of Implanted Radioactive Seeds in 3D TRUS Images for Intraoperative Prostate Brachytherapy.* 2006.

14. **Hough, P., V., C,.** Machine analysis of bubble chamber pictures. 1959, pp. 554-556.

15. **Duda, R., O.; Hart, P., E.;.** Use of the Hough transformation to detect lines and curves in pictures. s.l. : Communications of the ACM, 1972, Vol. 15, pp. 204-208.

16. **Wen, X.; Salcudean S.E.** Detection of Brachytherapy Seeds Using 3D Ultrasound. 2008, Vol. 8, pp. 855-858.

17. **Lee, J.; Labat, C.; Jain A.,K.; Song D.,Y.; Burdette, E.,C.; Fitchinger, G.; Prince, J.,L.** *Optimal matching for prostate brachytherapy seed localization with dimension reduction.* s.l. : Med. Image Comput. Assist. Interv. , 2009, Vol. 12, pp. 59-66.

18. **Dubois, D., F.; Prestidge B., R.; Hotchkiss, L., A.; Bice W.,S.; Prete, L., L.** Source localization following permanent transperineal prostate interstitial brachytherapy using magnetic resonance imaging. 1997, Vol. 39, pp. 1037-41.

19. **Rena, J., L.; Hyunsuk S.; Kyung, J.,L.; Soome, L.,Yookyung, K.; Sungkyu, K.; Jihno C.** [ed.] J. Korean Med. Sci. *A magnetic-resonance-based seed localization method for I-125 prostate implants.* 2007, Vol. 22, pp. 129-133.

20. **Wen, X.; Salcudean, S., E.** *Detection of brachytherapy seeds using 3D ultrasound.* s.l. : Conf. Proc. IEEE Eng. Med. Biol. Soc., 2008, pp. 855-858.

Acronyms

TRUS: Transpectral Ultrasound

US: Ultrasound

1D: 1-Dimensional

2D: 2-Dimensional

3D: 3-Dimensional